Journal of Biomedical Optics

SPIEDigitalLibrary.org/jbo

Acoustically penetrable optical reflector for photoacoustic tomography

Zijian Deng
Honghong Zhao
Qiushi Ren
Changhui Li

SPIE

Acoustically penetrable optical reflector for photoacoustic tomography

Zijian Deng, Honghong Zhao, Qiushi Ren, and Changhui Li
Peking University, College of Engineering, Department of Biomedical Engineering, Beijing 100871, China

Abstract. Photoacoustic tomography (PAT) detects ultrasound signals generated by the objects after absorbing illuminating photons. However, the widely used piezoelectric ultrasound transducers are generally not optically transparent, which would cause conflicts between the light illumination and the ultrasonic detection in PAT. We report a different acoustically penetrable optical reflector (APOR) concept to provide a solution to this conflict. We measured the properties of an APOR and experimentally tested its performance in a PAT system. The results demonstrated that the APOR successfully allowed the transducer to detector photoacoustic signals without affecting the light illumination. Moreover, the APOR concept can be readily implemented in various PAT systems. [DOI: 10.1117/1.JBO.18.7.070503]

Keywords: photoacoustic tomography; small animal imaging; optical imaging.

Paper 130337LR received May 20, 2013; revised manuscript received Jun. 20, 2013; accepted for publication Jun. 27, 2013; published online Jul. 9, 2013.

Photoacoustic tomography (PAT; also called optoacoustic tomography) is an emerging hybrid biomedical imaging method that combines optical contrast with ultrasonic detection.[1–4] Unlike other pure optical imaging modalities, PAT detects ultrasound signals generated through thermal expansion after the tissue absorbs the exciting electromagnetic energy. Over the past decade, PAT has made significant progresses and has been implemented into a vast range of biomedical research fields. Many PAT systems, such as photoacoustic (PA)-computed tomography and PA microscopy, have been developed.[3–5]

Every PAT system has two basic parts: light illumination and ultrasonic detection. In several cases, the light illumination path can have no overlap with the route of the ultrasound wave to the detector, such as the orthogonal PAT design,[6] and the transmission mode or dark-field PA microscopy.[7–9] However, many other kinds of PAT systems desire that the light and ultrasound waves a share common route in order to optimize the light delivery to the region of interest and perform accurate quantitative imaging. For instance, side illumination and detection alignment were commonly employed to image deeper internal organs,[10–14] while opaque transducers could partially block the illumination light. The blockage of light not only leads to ununiformed or unoptimized illumination but also changes the illumination condition during imaging that will hinder the quantitative imaging. Several ways have been explored to meet this issue. One way is to use optically transparent ultrasound transducers,[15,16] like the transducer made of Fabry–Perot polymer film.[15] These optical ultrasonic sensors currently require specific detection geometries (such as planar detection geometry), limiting their applications compared with those using the more flexible piezoelectric transducers. In addition, other methods relying on the reflection of light or ultrasound on a solid-liquid interface or the coating on a solid boundary have been used in PAT.[17–20] However, the large difference in the acoustic impedance causes significant ultrasound loss due to reflection, and it is also practically inconvenient to detect the reflected ultrasound.[19] Recently, a new design based on the dark-field illumination was used to bypass the opaque transducer array,[21] which provided a solution for PAT systems of the ring-based type.

In this article, we present a novel concept to resolve the conflict in transportation between the light and the ultrasound. Our design employs an acoustically penetrable optical reflector (APOR). Compared to conventional optical reflectors, the APOR is made of acoustically penetrable materials, such as the thin polyethylene (PE) or low-density polyethylene (LDPE) soft plastic membranes. On the soft plastic membrane, there is a very thin optical reflecting layer that enables it to be a good optical reflector with minor effect on the ultrasound transmission [as seen in Fig. 1(a)]. Due to the similar acoustic impedances between the membrane materials and water, as well as the thin thickness, both the acoustic reflection and attenuation can be minimized. Hence, APOR have two characteristics: optical reflection and high acoustical penetration.

Making an optical reflecting layer on thin membranes to reflect light is a mature technique. Here, we chose one common aluminum foil bag to make APOR. The material, as seen in Fig. 1(b), is made of polyethylene terephthalate/polyamide/aluminum/PE with a total thickness of 80 μm. An aluminum layer is sandwiched in the middle. We experimentally measured the optical reflectance and ultrasound penetration properties of this material.

Figure 2 shows the acoustic and optical properties of the chosen APOR material. The acoustic transmission of APOR depends on the incident angle. Figure 2(a) showed the relationship between the incident angle and the amplitude of the transmitted ultrasound by smoothing spline fit. Besides the acoustic transmission property, the spectrum of the transmitted signal with and without the APOR by using a cylindrical focused transducer with 10 MHz center frequency (V311, Olympus NDT, Inc., Waltham, Massachusetts) was also calculated in Fig. 2(b), which demonstrated that this APOR material has a negligible filtering effect. In addition to the acoustic property, the optical reflection coefficient was measured to be about 0.78 for current APOR material at 532-nm wavelength. All these properties can be further improved by using more appropriate materials.

Then, we employed this APOR in a circular scanning single-element PAT system, as shown in Fig. 3(a). In this setup, the APOR material was bent to form a "bowl-like" shape enclosing the object as in Fig. 3(b); the ultrasonic transducer circularly scanned around the outer wall of the APOR. An Nd:YAG laser (LS-2137/2, LOTIS TII, 532 nm, Minsk, Belarus), with

Address all correspondence to: Changhui Li, Peking University, College of Engineering, Department of Biomedical Engineering, Beijing 100871, China. Tel: +86-10-62767894; Fax: +86-10-62767894; E-mail: chli@pku.edu.cn

0091-3286/2013/$25.00

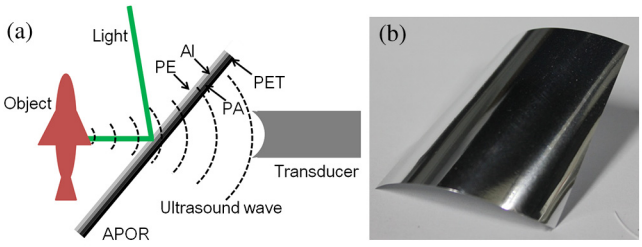

Fig. 1 (a) The concept of the APOR. (b) The photograph of an APOR material.

16-ns pulse duration and 10-Hz pulse repetition rate, was used as an irradiation source. The laser beam was first reflected by a cone mirror to form a ring-shaped light, which was then reflected by APOR and shone on the object surface inwardly at a horizontal plane. According to Fig. 2(a), about 0.79 amplitude of ultrasound could transmit the APOR at the current alignment (ultrasound incident angle of 32.66 deg). Owing to the unique property of APOR, the PA signals passed through the APOR and were detected by the cylindrical focused transducer at the same height without any conflicts. The measurement in plane and z-axial resolutions of the PAT system is about 100 and 400 μm, which are determined by the bandwidth and the geometric focusing of the transducer, respectively.

We imaged an adult Zebra fish using this PAT system equipped with the APOR. The adult zebra fish was euthanized by putting it in ice water before imaging. A transparent agar column (2% agar and 98% water) with a hole filled with water was made, and the adult Zebra fish was vertically placed in the hole, as shown in Fig. 3(a). The z position of the agar column can be adjusted by a lifting stage. The illuminating plane was fixed to the height of the focusing plane of the transducer.

The agar column containing the zebra fish was moved in the z-direction at even steps of 2 mm. Six planes from the center of body to the fish head were chosen for imaging with a total scanning length of 10 mm. Figure 4(a)–4(f) showed the imaging slices acquired at 532 nm without using any contrast agents, and a histology slice [Fig. 4(h)] corresponding to Fig. 4(f) was also provided.[22] According to the imaging results, the eyes, gills, ventral fins, and one major vessel were all clearly reconstructed. There are "circle-like" patterns in Fig. 4(a)–4(c), which were likely caused by the ultrasound reflection by the air-filled swim bladder. This result demonstrated that APOR performs successfully in PAT system to provide high quality imaging. The acquired signal from the transducer was amplified by 30 dB with a high-pass filter of 1 MHz.

The imaging quality highly depends on the quality of the optical reflecting layer of APOR and the cone mirror. In this article, a piece of food bag was selected to make the APOR, and the cone mirror was made by a machine shop, which has low optical quality and reduced the illumination efficiency in experiments. Replacing them with high optical quality parts will greatly improve the system.

In summary, APOR readily resolves the conflict between the light illumination and the ultrasonic detection for many PAT systems. Thus, without hindering the light transportation by opaque transducers, light illumination condition on target stays unchanged during the imaging, which is also significantly important for quantitative PAT imaging. Although we used a bowl-like shape for single-element circular scanning PAT system in this article, the APOR concept makes the patterns of light illumination that can be manipulated by using various

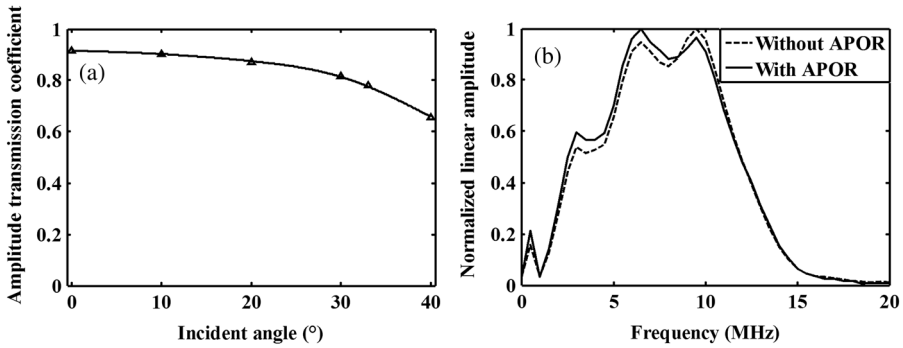

Fig. 2 The acoustic property of APOR. (a) The amplitude transmission coefficient versus the incident angle (using smoothing spline fitting method) and (b) the frequency spectrum of pulse-echo ultrasound signals with and without APOR membrane.

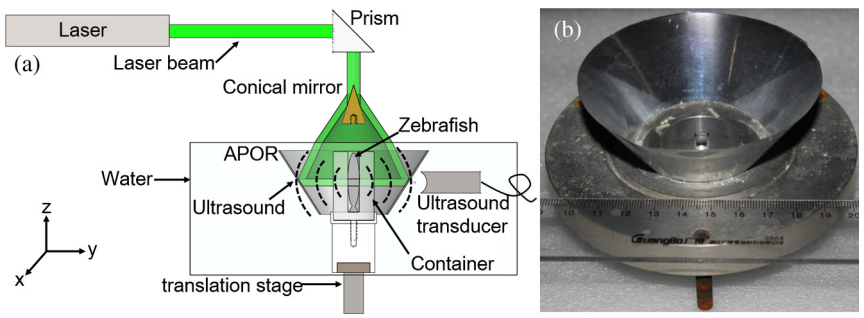

Fig. 3 A PAT system using APOR. (a) The schematic design diagram and (b) a photograph of the "bowl-like" APOR.

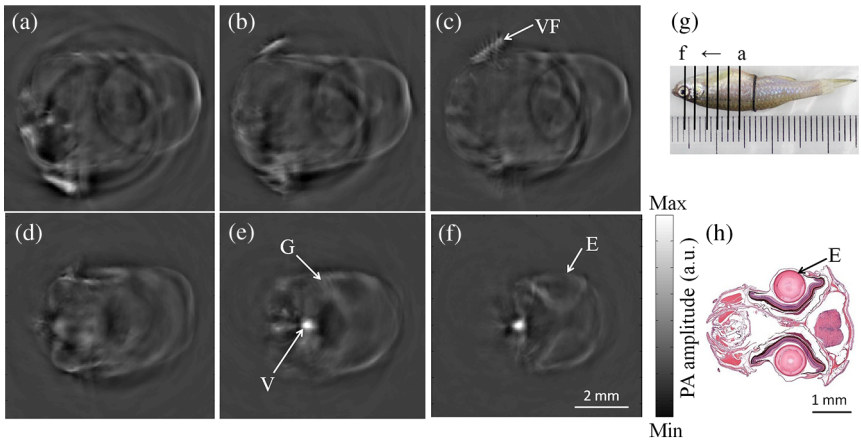

Fig. 4 Animal experiment results. (a)–(f) Cross-section PAT images of zebrafish [indicated as black lines in (g)]: E, eyes; G, gills; VF, ventral fins; V, vessel. (g) Photograph of the zebrafish. (h) Hematoxylin-eosin (HE) slice staining of zebrafish (http://zfatlas.psu.edu/view.php?atlas=18&s=207).

APOR designs without affecting the ultrasonic detection, which allows this APOR concept to be readily used in other PAT systems.

Acknowledgments

The authors appreciate Ms. Xiaoyun Jiang's instruction of mechanical design for the PAT system and Ms. Ran Yang's help on providing zebrafish. This work was sponsored by National Natural Science of China (Grant No. 61078073) and the National Basic Research Program of China (973 Program, 2011CB707502).

References

1. M. Xu et al., "Photoacoustic imaging in biomedicine," *Rev. Sci. Instrum.* **77**(4), 41101–41122 (2006).
2. A. Oraevsky et al., "Optoacoustic tomography," in *Biomedical Photonics Handbook*, T. Vo-Dinh, Ed., pp. 34–31, CRC, Boca Raton, Florida (2003).
3. C. Li et al., "Photoacoustic tomography and sensing in biomedicine," *Phys. Med. Biol.* **54**(19), R59–R97 (2009).
4. P. Beard, "Biomedical photoacoustic imaging," *Interface Focus* **1**(4), 602–631 (2011).
5. L. V. Wang et al., "Photoacoustic tomography: *in vivo* Imaging from organelles to organs," *Science* **335**(6075), 1458–1462 (2012).
6. X. D. Wang et al., "Noninvasive laser-induced photoacoustic tomography for structural and functional *in vivo* imaging of the brain," *Nat. Biotechnol.* **21**(7), 803–806 (2003).
7. C. Zhang et al., "Subwavelength-resolution label-free photoacoustic microscopy of optical absorption in vivo," *Opt. Lett.* **35**(19), 3195–3197 (2010).
8. S. Ye et al., "Label-free imaging of zebrafish larvae *in vivo* by photoacoustic microscopy," *Biomed. Opt. Express* **3**(2), 360–365 (2012).
9. K. Maslov et al., "*In vivo* dark-field reflection-mode photoacoustic microscopy," *Opt. Lett.* **30**(6), 625–627 (2005).
10. H.-P. Brecht et al., "Whole-body three-dimensional optoacoustic tomography system for small animals," *J. Biomed. Opt.* **14**(6), 064007 (2009).
11. M. R. Chatni et al., "Tumor glucose metabolism imaged *in vivo* in small animals with whole-body photoacoustic computed tomography," *J. Biomed. Opt.* **17**(7), 076012 (2012).
12. R. Su et al., "Three-dimensional optoacoustic imaging as a new non-invasive technique to study long-term biodistribution of optical contrast agents in small animal models," *J. Biomed. Opt.* **17**(10), 101506 (2012).
13. R. Ma et al., "Non-invasive whole-body imaging of adult zebrafish with optoacoustic tomography," *Phys. Med. Biol.* **57**(22), 7227–7237 (2012).
14. X. D. Wang et al., "Imaging of joints with laser-based photoacoustic tomography: an animal study," *Med. Phys.* **33**(8), 2691–2697 (2006).
15. J. Laufer et al., "*In vivo* photoacoustic imaging of mouse embryos," *J. Biomed. Opt.* **17**(6), 06122 (2012).
16. G. Paltauf et al., "Photoacoustic tomography using a Mach-Zehnder interferometer as an acoustic line detector," *Appl. Opt.* **46**(16), 3352–3358 (2007).
17. L. D. Wang et al., "Fast voice-coil scanning optical-resolution photoacoustic microscopy," *Opt. Lett.* **36**(2), 139–141 (2011).
18. K. Maslov et al., "Optical-resolution photoacoustic microscopy for *in vivo* imaging of single capillaries," *Opt. Lett.* **33**(9), 929–931 (2008).
19. L. G. Montilla et al., "Real-time photoacoustic and ultrasound imaging: a simple solution for clinical ultrasound systems with linear arrays," *Phys. Med. Biol.* **58**(1), N1–N12 (2013).
20. S. Hu et al., "Second-generation optical-resolution photoacoustic microscopy with improved sensitivity and speed," *Opt. Lett.* **36**(7), 1134–1136 (2011).
21. J. Xia et al., "Whole-body ring-shaped confocal photoacoustic computed tomography of small animals in vivo," *J. Biomed. Opt.* **17**(5), 050506 (2012).
22. "Zebrafish Atlas," http://zfatlas.psu.edu/, NIH grant 5R24 RR01744, Jake Gittlen Cancer Research Foundation and PA Tobacco Settlement Fund (12 November 2012).